Transport cost of a high energy efficiency hybrid robot

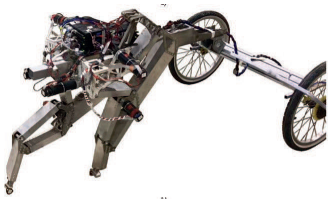

Costo de transporte de un robot híbrido de alta eficiencia energética

Francisco-Javier López-Lombraña, Angel-Gaspar González-Rodríguez, Antonio González-Rodríguez, David Rodríguez-Rosa, Guillermo Rubio-Gómez, Sergio Juárez-Pérez, Fernando-Jose Castillo-García
Escuela de Ingeniería Industrial de Toledo. Av. Carlos III, Real Fábrica de Armas – 45071 Toledo (España)

DOI: https://doi.org/10.6036/9828 Received: 17/06/2020 • Reviewing: 10/07/2020 • Acepted: 22/09/2020

To cite this article: LÓPEZ-LOMBRAÑA, Francisco-Javier; GONZÁLEZ-RODRÍGUEZ, Ángel-Gaspar; GONZÁLEZ-RODRÍGUEZ, Antonio; RODRÍGUEZ-ROSA, David; RUBIO-GÓMEZ, Guillermo; JUÁREZPÉREZ, Sergio; CASTILLO-GARCÍA, Fernando-José. TRANSPORT COST OF A HIGH ENERGY EFFICIENCY HYBRID ROBOT. DYNA, Marzo 2021, vol. 97, no. 2, 6 pp. DOI: https://doi.org/10.6036/9828

RESUMEN

- El costo del transporte es uno de los parámetros más importantes para estudiar la eficiencia y autonomía de operación de un robot caminante. Este análisis tiene en cuenta factores como el peso, consumo de los actuadores, velocidades, aceleraciones, superficies de trabajo, modelo de ciclo de pasos, etc. que deben estudiarse en detalle para producir una locomoción estable y energéticamente eficiente. Este artículo presenta los resultados obtenidos para el costo de transporte de un robot híbrido de dos patas delanteras más dos ruedas traseras con un peso total de 50 kg en diferentes escenarios. El costo de transporte del robot híbrido propuesto se obtiene realizando un análisis detallado de la cinemática, dinámica, estabilidad y consumo de energía. Se ha obtenido un valor satisfactorio de eficiencia, en términos de costo de transporte, debido a un diseño gravitacionalmente desacoplado de las patas. El costo de transporte del robot obtenido se mueve entre 0,11 y 0,24, dependiendo del entorno de trabajo en el que actúe, con un valor de 0,18 para las condiciones nominales, esto es, caminando en un plano horizontal liso sin carga adicional. Este trabajo presenta un nuevo diseño de una pata robótica desacoplada gravitacionalmente mediante un nuevo esquema en el que dicha pata se compone de tres mecanismos de cuatro barras que se pueden sintetizar de forma independiente. Dichos mecanismos implican movimiento frontal y vertical dentro del mismo plano detrabajo. Un mecanismo genera una trayectoria horizontal para remolcar el robot, mientras que otro genera una trayectoria vertical, y un tercero tiene la misión específica de hacer que la velocidad de remolque sea constante cuando el motor correspondiente opera, también, a una velocidad constante,
- Palabras Clave: tecnologías de asistencia, localización GPS, movilidad de personas invidentes, estimulación podotáctil, interfaz vibrotáctil, sistema vestible.

ABSTRACT

Purpose - The cost of transport is one of the most important values to the efficiency and operation autonomy of a walking robot. This analysis involves factors as the weight, consumption of the actuators, speeds, accelerations, work surfaces, step cycle model or distance travelled, which must be studied in detail to produce stable and energy-efficient locomotion. This paper presents the results obtained for the cost of transport of a hybrid robot with two front legs and two rear wheels, with a total weight of 50 kg in different scenarios. Methodology/approach - The transportation cost of the proposed hybrid robot is obtained by carrying out a detailed analysis of the kinematics, dynamics, stability and energy consumption. Findings - A satisfactory value of efficiency has been obtained, in terms of cost of transport, owing to a gravitationally decoupled design of the legs. The cost of transport of the robot proposed is between 0.11 and 0.24, depending on the work environment in which it operates, that is, walking on a smooth horizontal plane without additional load. Originality/value – This work presents a new design of a gravitationally decoupled robotic leg by means of a new scheme in which the leg is composed of three four-bar mechanisms that can be synthesized independently. These three mechanisms involve frontal and vertical movement within the same plane of movement. One mechanism generates a horizontal path for tow, while another generates a vertical path and a third has the specific mission of making the tow velocity constant when the corresponding motor is operated at a constant velocity. The overall goal of the mechanisms is to improve robot's efficiency.

Key words: Cost of transport, gravitationally uncoupled motion, energy efficiency, experimental validation, hybrid robot.

1. INTRODUCTION

Although the most widespread type of locomotion for mobile robots is wheel driven [1], the development of legged robots has increased significantly in the last few years owing to the improvements made in actuator control and efficiency algorithms, among others. It is currently necessary to consider the advantages, in terms of efficiency, of wheeled robots, for flat surfaces, compared to those with legs [2]. One example of this is the planetary exploration robots such as the Sojourner, Spirit, Opportunity and Curiosity. or the nuclear accident that occurred in Fukushima in 2011, in which human access was restricted and it was necessary to use the PackBot and Warrior robots for rescue operations [3] supervision.

However, robots with paws are more suitable for applications running on uneven terrain [4], harmful to humans or when robots of relative small size are needed [5] such as those needed for home applications [6] and to help older people [7].

Another factor that has contributed to the proliferation of such robots is that of being able to give them an animal appearance [8] or humanoid [9]. This appearance helps its development, as it allows us to imitate its namesakes of the animal kingdom to investigate and better understand its locomotive behavior.

In the case of robots with paws, the combined structure of muscles, joints and tendons is still far from being successfully imitated.

This is noted because, although electric motors are more efficient than muscles, the cost of global transport is still considerably higher in the case of robots.

Most actuators are not capable of transforming kinetic energy into electric or potential of any kind, signifying that, the negative power resulting from stop actions within each step cycle cannot be recovered [10]. On the contrary, the corresponding actuator must expend energy to cancel the kinetic energy of the paw in order to be able to slow it down.

Another difficulty for paws robots, relative to wheel drive robots, is the increased complexity of the control algorithm required [11] and the lower accuracy of odometric position indicators. In addition, the existence of numerous degrees of freedom, variables involved, different dynamic and inertial situations, which require a greater number of calculations [12] carries a much higher computational cost [13].

The first successful designs of robots with paws that achieved high locomotion efficiency rates correspond to Dynamic Passive Robots (PDW) [14], able to move without any external energy input [15]. With the right joint-link structure, a slight downward slope, a simple push and the force of gravity, these mechanisms can walk for theoretically infinite time [16]. Since then many improvements have been achieved in terms of control, mechanics, physical and mathematical models, materials, etc. These advances have led to the latest prototypes of bipedal robots, quadrupeds, etc., which are able to walk autonomously, not only maintaining balance, but also moving on all kinds of surfaces containing a multitude of obstacles [17].

2. GRAVITATIONALLY DECOUPLED LEG DESIGN. START-UP

This paper presents optimal results, in terms of transport cost, thanks to a method that optimizes the horizontal and vertical movements of the DOGO II robot's leg [18], which has been used as the base for the hybrid robot front train of this job. Side movement is essential to maintain stability [19] and being able to rotate, but gravitationally decoupling this mechanism will generate weight gain without necessarily achieving an improvement in efficiency. The lateral movement is, therefore, performed with a simple hinge joint whose axis of rotation is shown in Figure 1, located at point H.

Three four-bar mechanisms are used to efficiently decouple vertical and horizontal movements. The final configuration is shown on the left-hand side of Figure 1. On the right-hand side of this figure are the three segregated mechanisms in which such a configuration can be broken down.

Mechanism A in Figure 1 is a four-bar mechanism that has been synthesized in order to generate a rectilinear path for point P (foot tip that rests on the ground) following the procedures indicated in [20].

A natural and efficient walking cycle requires that the speed of the leg be constant during the drag movement. To facilitate control and minimize losses from accelerations and decelerations of the motors, there must be a proportionality between the speed of the motor that causes the horizontal movement of the leg and the final speed of the end of the leg. In this way, to achieve the desired horizontality of the drag movement and a movement at constant speed, the authors propose to use two mechanisms of four independent bars. This is the reason for adding the mechanism labeled B in the Figure 1.

In order to establish the objective function of mechanism B, the leg end of mechanism A has been placed in a series of equidistant positions P1Q2Q3,..., Pn. In these positions, bar A2 adopts the angular positions A21, A22, A23,..., A2m, which are not separated by equal angles. Bar A2 is the input bar for the four-bar mechanism A, but it is also attached to bar B4, which is the output bar of the four-bar mechanism B. This angular rotation function of bar B4 (or A2) will be the function synthesized by the four-bar mechanism labeled B. The motor that provides horizontal movement to the leg drives the B2 bar.

With this configuration, when the motor in B2 rotates at a constant speed, mechanism B transforms it into the function that makes the movement of the point P of the coupler A3 move with approximately constant speed.

Finally, the four-bar mechanism C is added to the coupler of mechanism A (labeled A3) in order to provide the vertical leg movement at point P of the coupler, labeled C3. This mechanism has been synthesized to generate a vertical trajectory using the same optimization method used in mechanism A, although logically mechanisms A and C are geometrically different because they have different geometric restrictions. The motor that drives the vertical movement of point P moves the C2 bar of the mechanism.

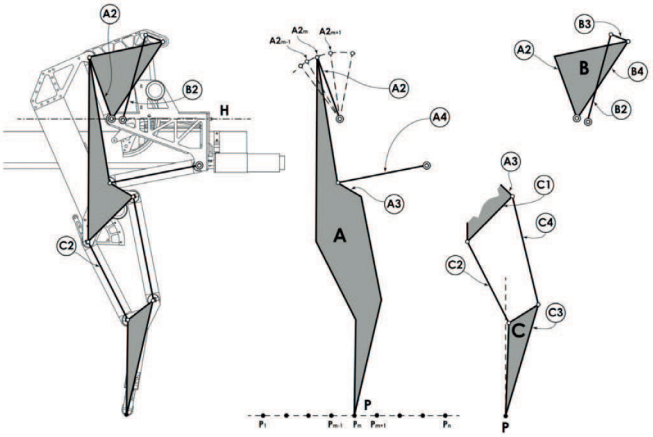

Fig. 1: Gravitationally Decoupled Leg Configuration

This design, together with an open loop control scheme, significantly simplifies the control when walking. It also makes it more robust in situations other than design.

From the mechanical point of view, the present proposed design has the following advantages [2]:

- Reduced inertia, and the wiring of the actuators is located on the hip or close to it, away from the point of contact with the ground.The reliability of the joints has improved, since the actuators are not in the trajectories where impacts and support reactions occur.
- The cost of the robot presented is drastically reduced thanks to the use of a gear reducer and a rach-and-pinion mechanism in the actuators. It is possible to include hydraulic actuators for scaling.
- Like mammals, the connection between the paw and the hip is vertical, rather than lateral as in reptiles or insects [21]. This improves the load capacity and reduces the width.
- Rubber supports have been added at the ends of the paws, wich are in contact with the surface, in order to prevent slips, thus relieving impacts.

The assembled set of two front drive legs plus two rear free wheels is shown in the Figure 2.

2.1. DESIGN AND HARDWARE

The front powertrain consisting of two legs, shown in Figure 2, is taken from the dogo II quadrupedal robot [18]. In addition, on this robot, the hind legs were replaced by two free wheels involving a considerable reduction in weight, from 84 to 50 kg. The Figure 2B shows the final appearance of the prototype, where each leg has three degrees of freedom.

This hybrid system is controlled so that, in its walking action, it is always supported on a minimum of three points (two wheels plus one leg), thus forming a triangle of stability. To do this, the wheels have separated from each other a distance of 850 mm. and distanced from the front legs so that the CG of the assembly is always within that triangle, not being compromised its support and stability. The most unfavourable situation, in terms of equilibriu, can be seen in the Figure 3, being able to observe how the CG remains within the aforementioned stability triangle.

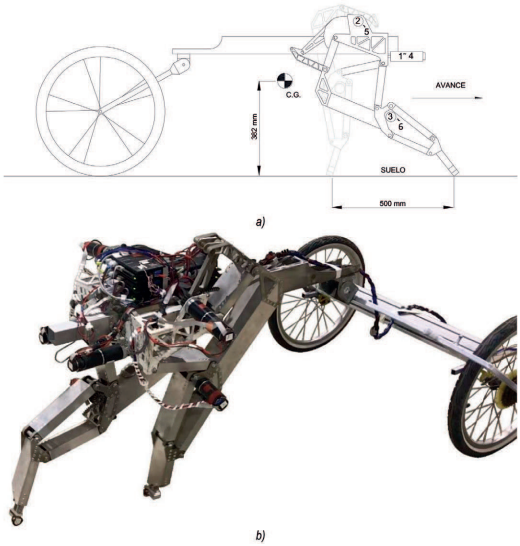

Fig. 2: Hybrid robot. a) Right side view; b) Final appearance

Figure 3 shows the corresponding location of the engines, on their right side M1, M2 and M3, being their namesakes on the side M4, M5 and M6.

2.2 CONTROL STRUCTURE

The control scheme has two levels: a higher level that, formed by a microcontroller, executes the program that commands the trajectories to be followed by the different actuators by launching them in a coordinated manner; and a lower level consisting of EPOS control cards responsible for operating the engines according to the trajectories generated at the top level.

Each step cycle can be seen as a discrete event process with easily identifiable transitions, which are achieving the definition of the target position and its corresponding motion action in open buble.

3. EXPERIMENTAL VALIDATION AND RESULTS

This section details the experimental results as regards the energy efficiency of DOGO II robot [18], in its hybrid form.

3.1. SETTING UP EXPERIMENTS

The results obtained have been achieved at a speed of 1 m / 6260 ms by experimental tests of the following nature and condition:

- Smooth horizontal surface (printed concrete).
- Climbing a ramp (with a slope of 9%)
- Down a ramp (with a slope of -9%)
- Carrying a horizontal load of 42 kg.
- Irregular horizontal surface (ground).

A research assistant was responsible for operating the remote computer and for sending the instructions to the user interface. This first experiment did not require the use of the smartphone, cloud server, and remote computer.

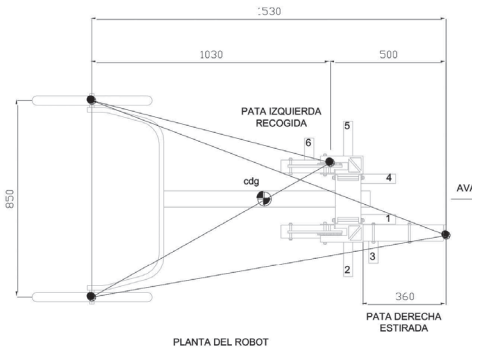

Fig. 3: Hybrid robot plant (dimensions in mm.). Stability

3.1.1. Nature of each cycle

It is important to clarify the cycle dynamics of each of the two legs, being identical to each other, but outdated in half cycle time. Each complete cycle consists of two steps. In the first semicycle the left leg moves backwards, causing the robot to advance, performing the same action on the right leg in the second semicycle. These two steps allow to cover a distance of one meter, which means that each leg advances half a meter. The actuator dynamics of each degree of freedom are parameterized as follows:

- Hip: This motor is responsible for the side movements of the robot, taking care of the opening or closing of the legs. For transport cost tests it has been maintained at a constant opening angle while the robot walks, implying that it does not influence such action as the various tests tested follow straight trajectories.
- Knee: This engine takes care of the robot's feed movement (50 cm. on each leg).
- Foot: This motor is responsible for coupling/uncoupling the foot with the contact surface. It rises / poses a distance of 3 cm.

3.2. INTERPRETATION OF RESULTS

The second experiment aimed at evaluating the performance of the AT system as a whole and at determining whether it can actually assist the mobility of blind pedestrians.

3.2.1. Electricity testing

In this section, the power consumption results of the M2, M3, M5 and M6 motors are shown in four Intensity (A) / Time(s) graphs during a full cycle. In each of them, the results of the same engine have been overlapned for each of the five tests carried out corresponding to different working environments, making their differences better visible. As mentioned above, the results of the M1 and M4 engines are not taken into account by not influencing the robot's walking action.

In the Figure 4 the instantaneous intensity value of the M3, M6, M2 and M5 engines is displayed for each of the tests performed. Those corresponding to the M3 and M6 engines represent the consumption of both feet. In these graphs it can be observed that a consistency is maintained in the results shown, showing how the shape of the curves corresponding to the different tests follows a certain pattern. Note how in the first half of the cycle the consumption of the M6 engine is higher than that of the M3 engine. This is because, in this first semicycle, it is the left foot that is in contact with the ground and therefore supporting the weight and inertial stresses of the robot due to its movement, while in the second part of the cycle the consumption of the M6 engine is reduced practically to zero since the foot it commands is in the flight phase. It can be seen how both graphs are symmetrical to a center point of the

graphs. This is because while one foot is in the flight phase (without any load) the other foot is in the support phase and vice versa.

The M2 and M5 engines are responsible for the knee movements that execute the robot's feed. In the first half of the cycle, the M5 engine is responsible for moving the robot forward 50 cm. with the left leg in contact with the ground, while the M2 engine keeps the right leg in the flight phase moving forward to position itself in the next step. In the second half of the cycle, the same thing happens, but with the M2 and M5 engines changed. In these graphs, the differences in consumption between the different tests are best appreciated because their actions require a different effort. In the ramp climb test you can see an increase in consumption because, logically, the robot now has against gravity in its advance.

3.2.2. Power consumption

During the different tests, in real time, readings of intensity, time and speed (linked to the voltage) have been made that have allowed us to develop the graphs and above all to be able to Calculate real energy consumption in each work environment, by expression (1):

$$E = \sum P(t) \cdot \Delta t \quad (1)$$

where t is the elapsed time between the readings and P(t) is the power consumed in that time period, which is calculated according to the expression (2):

$$P(t) = V(t) \cdot I(t) \quad (2)$$

Finally, total consumption is obtained by expression (3):

$$\sum_{p=1}^{np} \sum_{k=1}^{nm} Epk \quad (3)$$

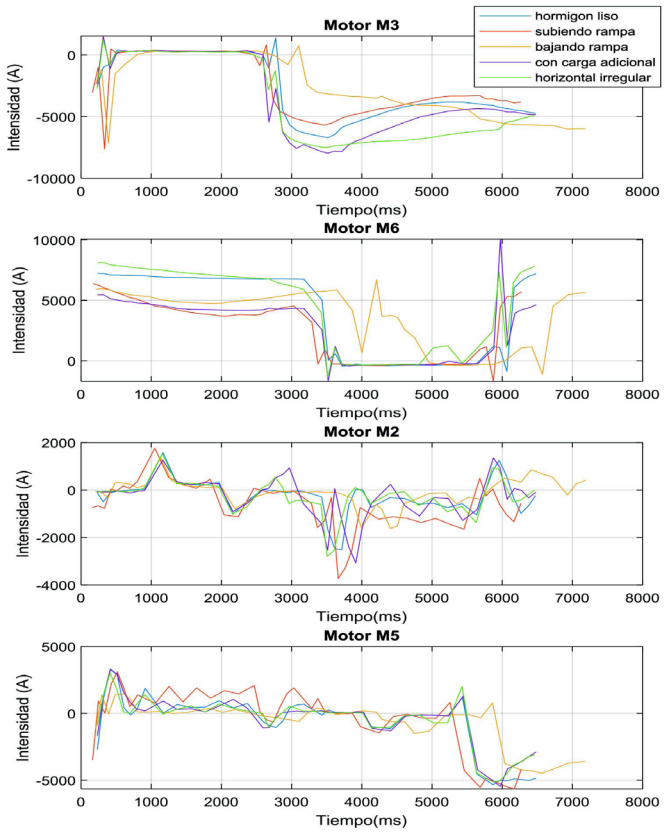

Fig. 4: Current consumed / time on M3, M6, M2 and M5 engines.

Where N_0 It is the number of movement phases per cycle, N_M The number of engines involved and E_{Pk} energy consumed, calculated at (1) for the *Q* and the engine *K:i.*

Stage	Energy consumed
Smooth horizontal surface	887.39 J
Climbing a ramp (slope s 9%)	1201.75 J
Lowering a ramp (slope -9%)	824.01 J
Carrying an additional load of 42 kg.	995.99 J
Irregular horizontal surface	972.18 J

Table 1: Energy consumed in each work scenario

The Table 2 shows the percentages of consumption of the actuators who are in the flight phase and those who are in the support phase in each scenario. It can highlight the following:

- In the tests carried out in horizontal surfaces, regardless of their nature, it is observed how the consumption of the flight and ground phases are very similar. This is because, although more effort is required in the ground phase by the single engine that performs the advance (engine 2 or 5, depending on which semicycle we are in), the flight phase involves a greater number of engines with a greater number of starts and stops that mean that consumption tends to rise and match the ground phase. There is a somewhat greater difference between flight and ground consumption in the irregular horizontal surface because while the leg that is in contact with the terrain performs the forward manoeuvre there are situations of sliding between that leg and the surface which means that it actually advances slightly less than intended and therefore its consumption in the ground phase is somewhat less proportionally than in the rest of the tests on horizontal planes.
- In the test of Rise, however, it is seen how the percentage of consumption in the support phase is higher than the other tests, since the force of gravity is negatively involved.
- In the test of Down, happens just the opposite of the rise as the force of gravity plays in favor of the downward trajectory.
- In the test with a additional load of 42 kg., as expected, consumptions, in absolute terms, are higher than those of the smooth horizontal surface test without load, as more effort must be made. However, in terms of percentage it is seen how in the soil phase consumption is somewhat lower. This is due to small slippages between the tip of the foot and the surface which results in a little less real route terrain and therefore lower consumption.

3.2.3. Cost of transportation

Gabrielli and von Karman [22] introduce for the first time the concept of energy efficiency during locomotion, based on the same idea as the cost of transportation defined by Collins [23], where, for walking robots, the formula is followed (4) Adimensional:

$$\varepsilon = \frac{E}{M \cdot g \cdot d} \quad (4)$$

Stage	Energy consumed in flight phase (July%)	Energy consumed in support phase (July %)	Total energy consumed (July %)
Smooth horizontal surface	441,36 (49,73%)	446,03 (50,27%)	887,39 (100%)
Climbing a ramp (slope s 9%)	468,36 (38,97%)	733,39 (61,03%)	1201,75 (100%)
Lowering a ramp (slope -9%)	476,88 (57,87%)	347,13 (42,13%)	824,01 (100%)
Carrying an additional load of 42 kg.	510,95 (51,30%)	485,04 (48,70%)	995,99 (100%)
Irregular horizontal surface	517,03 (53,18%)	455,15 (46,82%)	972,18 (100%)

Table 2 : Table of percentages of consumption in the flight and support phases

Where E is total energy consumption for a distance traveled D (10 m in all tests), M is the mass of the robot and G is the acceleration of gravity.

The terms E And D they have a directly proportional relationship, that is, if the distance travelled increases proportionately the energy consumed used to travel that distance, so the distance travelled alone does not imply a variation in the cost of transport. The same goes for the term M. Increasing mass also means consumption E, causing the cost of transportation [24], do not vary significantly.

Within the energy efficiency, we can distinguish two types: one for the mechanical cost of transportation,M, if only the positive work of the actuators is considered, and another for the electrical cost of transport,E, if the total electrical energy consumed by the system is used. This article uses the latter type.

Using the results shown in the previous section, the electric cost of transportation obtained for each scenario is shown in the Table 3.

Stage	E_E
Smooth horizontal surface	0,1809
Climbing a ramp (slope s 9%)	0,2425
Lowering a ramp (slope -9%)	0,1678
Carrying an additional load of 42 kg.	0,1100
Irregular horizontal surface	0,1982

Table 3: Electric cost of transportation for each scenario

3.3. COMPARISON WITH OTHER ROBOTS OR SYSTEMS

Collins also provides data on transport costs of other robots, which are very useful in this document in terms of comparison. Some of them are shown in the Table 4. It is worth noting the scarcity of data in this regard, being very difficult to find them in other articles or publications.

Robot (system)	E_E
Our robot (DOGO II hybrid)	0,18
Lebrel Hybrid Robot	0,18
Bipedal Cornet	0,20
Human	0.20
MIT's Spring Flamingo	2,80
Asimo bipedo	3,20
T.U. Delft's Denise	5,30

Table 4: Cost of transporting other robots or systems

For this reason, the results shown do not belong to robots of similar characteristics, but they serve to give us an idea of the range in which we are moving.

4. CONCLUSIONS

The attempt to improve efficiency is a constant in any area, being directly related to savings. This efficiency and, therefore, the cost of transport achieved for the hybrid robot used in this work has been achieved thanks to the mechanical and dynamic design of its leg.

This article introduces experimental validation, in terms of transportation cost, of a new mechanical design gravitationally decoupled.

Using, as a basis for experimentation, the front leg train of the DOGO II robot [18], and after developing a control architecture that executes an effective movement of the robot, electrical consumption readings of each actuator are recorded in different working scenarios, reaching the following conclusions:

- The use of this particular type of gravitationally decoupled leg leads to efficient movements and trajectories with as few actuators as possible. This has a positive impact on consumption. In addition, thanks to this structure, it is easier to establish corrections between changes made to the running conditions and the demand of the engines.
- Although the cost of transport is the best indicator to represent the energy efficiency of walking robots, this is a value rarely found in any type of literature, and, of the small number of existing references, none deals with a sufficiently profound impact on variations in this coefficient depending on different working environments. For this reason, the results shown in this work contribute to providing more information in this field.
- It is worth noting the efficiency values and transport costs obtained, thanks to a gravitationally decoupled design of the legs. The cost of transporting the hybrid robot presented varies between 0.11 and 0.24 depending on the working environment, being able to take a value of 0.18 for nominal conditions, that is, walking on a smooth horizontal plane without additional load.
- It is always positive to be able to compare your own experimental results with existing ones. To this end, it is desirable that such comparisons be made between more or less similar systems that allow for minimally precise conclusions. In this sense, only absolute values of robots or systems could be found without specifying under what conditions they were obtained. However, these values serve as guidance and we can see that the results achieved are competitive.
- Therefore, comparative data from the Table 4, while real, they cannot be interpreted beyond a reference to be taken into account, as they belong to systems and/or robots of typologies

not similar to our own. The most important objective was to experimentally validate the efficiency and cost of transport that can provide the leg mechanism presented in this work. Once tested in different environments, for a straight trajectory, that the results are optimal, these can be used for future research where you can change the current configuration of the robot, two front legs plus two free rear wheels (hybrid), to four legs (quadruped) making more complex trajectories with obstacles in which the balancing component will demand the use of more actuators.

- The experimental tests presented in this document show that the peculiarity of the mechanical and dynamic design of our hybrid robot is, compared to others, quite effective and, consequently, really efficient to act in different scenarios, thus being able to provide a service in those areas in which humans have restricted or prohibited access with an irregular orography where wheeled robots see their capabilities greatly diminished.

References

1] GARCIA, Elena, et al. The evolution of robotics research. IEEE Robotics & Automation Magazine, 2007, vol. 14, no 1, p. 90-103. https://doi.org/10.1109/mra.2007.339608

[2] GONZALEZ-RODRIGUEZ, Angel Gaspar; GONZALEZ-RODRIGUEZ, Antonio; CASTILLO-GARCIA, Fernando. Improving the energy efficiency and speed of walking robots. Mechatronics, 2014, vol. 24, no 5, p. 476-488. https://doi.org/10.1016/j.mechatronics.2014.05.004

[3] HIROSE, Shigeo; FUKUSHIMA, Edwardo F. Development of mobile robots for rescue operations. Advanced Robotics, 2002, vol. 16, no 6, p. 509-512. https://doi.org/10.1163/156855302320535845

[4] KALAKRISHNAN, Mrinal, et al. Fast, robust quadruped locomotion over challenging terrain. En 2010 IEEE International Conference on Robotics and Automation. IEEE, 2010. p. 2665-2670. https://doi.org/10.1109/robot.2010.5509805

[5] MORREY, Jeremy M., et al. Highly mobile and robust small quadruped robots. En Proceedings 2003 IEEE/RSJ International Conference on Intelligent Robots and Systems (IROS 2003)(Cat. No. 03CH37453). IEEE, 2003. p. 82-87. https://doi.org/10.1109/iros.2003.1250609

[6] LOHSE, Manja; HEGEL, Frank; WREDE, Britta. Domestic applications for social robots: an online survey on the influence of appearance and capabilities. 2008. https://doi.org/10.14198/jopha.2008.2.2.04

[7] TANG, Dalai, et al. A novel multimodal communication framework using robot partner for aging population. Expert Systems with Applications, 2015, vol. 42, no 9, p. 4540-4555. https://doi.org/10.1016/j.eswa.2015.01.016

[8] ZHANG, Si, et al. Trot pattern generation for quadruped robot based on the ZMP stability margin. En 2013 ICME International Conference on Complex Medical Engineering. IEEE, 2013. p. 608-613. https://doi.org/10.1109/iccme.2013.6548322

[9] VANDERBORGHT, Bram, et al. Development of a compliance controller to reduce energy consumption for bipedal robots. Autonomous Robots, 2008, vol. 24, no 4, p. 419-434. https://doi.org/10.1007/s10514-008-9088-5

[10] MADDEN, John D. Mobile robots: motor challenges and materials solutions. science, 2007, vol. 318, no 5853, p. 1094-1097. https://doi.org/10.1126/science.1146351

[11] CAPPELLETTO, Jose, et al. Gait synthesis and modulation for quadruped robot locomotion using a simple feed-forward network. En International Conference on Artificial Intelligence and Soft Computing. Springer, Berlin, Heidelberg, 2006. p. 731-739. https://doi.org/10.1007/11785231_76

[12] MISTRY, Michael; BUCHLI, Jonas; SCHAAL, Stefan. Inverse dynamics control of floating base systems using orthogonal decomposition. En 2010 IEEE international conference on robotics and automation. IEEE, 2010. p. 3406-3412. https://doi.org/10.1109/robot.2010.5509646

[13] PAOULLIS, Panagiotis. Algoritmos basados en matrices para resolver problemas estadísticos de alto coste computacional. 2017. Tesis Doctoral. Universidad de Oviedo.

[14] COLLINS, Steven H.; WISSE, Martijn; RUINA, Andy. A three-dimensional passive-dynamic walking robot with two legs and knees. The International Journal of Robotics Research, 2001, vol. 20, no 7, p. 607-615. https://doi.org/10.1177/02783640122067561

[15] DONELAN, J. Maxwell; KRAM, Rodger; KUO, Arthur D. Mechanical work for step-to-step transitions is a major determinant of the metabolic cost of human walking. Journal of Experimental Biology, 2002, vol. 205, no 23, p. 3717-3727.

[16] HONEYCUTT, Craig; SUSHKO, John; REED, Kyle B. Asymmetric passive dynamic walker. En 2011 IEEE International Conference on Rehabilitation Robotics. IEEE, 2011. p. 1-6. https://doi.org/10.1109/icorr.2011.5975465

[17] HU, Nan, et al. Trotting gait planning for a quadruped robot with high payload walking on irregular terrain. En 2014 International Joint Conference on Neural Networks (IJCNN). IEEE, 2014. p. 581-587. https://doi.org/10.1109/ijcnn.2014.6889549

[18] GONZÁLEZ LUCHENA, Iván. Design, manufacture and stability algorithm development of the quadruped robot Dogo II. 2015.

[19] GONZALEZ-LUCHENA, Ivan, et al. A new algorithm to maintain lateral stabilization during the running gait of a quadruped robot. Robotics and Autonomous Systems, 2016, vol. 83, p. 57-72. https://doi.org/10.1016/j.robot.2016.06.004

[20] RODRIGUEZ, Antonio Gonzalez; RODRIGUEZ, Angel Gonzalez; REA, Pierluigi. A new articulated leg for mobile robots. Industrial Robot: An International Journal, 2011. https://doi.org/10.1108/01439911111154090

[21] HIROSE, Shigeo, et al. Quadruped walking robots at Tokyo Institute of Technology. IEEE Robotics & Automation Magazine, 2009, vol. 16, no 2, p. 104-114. https://doi.org/10.1109/mra.2009.932524

[22] GABRIELLI, G. What price speed? Specific power required for propulsion of vehicles. Mechanical Engineering-CIME, 2011, vol. 133, no 10, p. 4-5.

[23] COLLINS, Steve, et al. Efficient bipedal robots based on passive-dynamic walkers. Science, 2005, vol. 307, no 5712, p. 1082-1085. https://doi.org/10.1126/science.1107799

[24] LARSEN, Jørgen Christian; STØY, Kasper. Locomotion: Energy Efficiency of Robot Locomotion Increases Proportional to Weight. En FETT11-The European Future Technologies Conference and Exhibition. 2011. https://doi.org/10.1016/j.procs.2011.09.083